



## Future climate impact of all-solid-state batteries

Shan Zhang<sup>a,\*</sup>, Daniel Brandell<sup>b</sup>, Mario Valvo<sup>b</sup>, Bernhard Steubing<sup>c</sup>, Åke Nordberg<sup>a</sup>

<sup>a</sup> Department of Energy and Technology, Swedish University of Agricultural Sciences, P.O Box 7032, SE-75007, Uppsala, Sweden

<sup>b</sup> Department of Chemistry - Ångström Laboratory, Uppsala University, Box 358, Uppsala, 751 21, Sweden

<sup>c</sup> Institute of Environmental Sciences (CML), Leiden University, 2300, RA Leiden, the Netherlands

### ARTICLE INFO

#### Keywords:

All-solid-state batteries  
Prospective life cycle assessment  
Future climate impact  
Emerging technologies

### ABSTRACT

All-solid-state batteries (ASSBs) are considered a next-generation technology with the potential to enhance the safety and extend driving range in electric vehicles. This study assesses the climate impact of two ASSB chemistries in 2025, 2030, 2040, and 2050, using a prospective life cycle assessment. The study accounts for changes in energy-intensive processes, secondary material use, and advances in battery design. A battery dimensioning model is developed to quantify material demand and the corresponding specific energies. The findings indicate that ASSB NMC811 with LLZO electrolyte likely has a higher climate impact than LIBs, while ASSB LFP with a polymer electrolyte has the potential to achieve impacts comparable to LIB LFP. Minimizing non-cathode materials significantly lowers the climate impact of ASSBs, making them comparable to LIBs. Key contributors to the climate impact of both ASSBs are the electrolyte and cathode active materials, with the anode and current collector also important in polymer-based ASSBs. The analysis also shows the availability of lanthanum may pose constraint on scaling LLZO based ASSBs.

### 1. Introduction

As society transitions toward a fossil-free economy, rechargeable batteries, especially for mobile applications, are becoming increasingly crucial. The recent drive toward vehicle electrification has highlighted the dominance of lithium-ion batteries (LIBs) in the electromobility sector, due to their high energy and power density, superior cycleability, and reliability. However, after years of development, LIBs are approaching their limits in energy density. They face several challenges in meeting the growing demand for extended driving ranges in electric vehicles (EVs), primarily due to the limited capacities of graphite anodes and transition metal oxide cathodes (Tang et al., 2021), which remain the most constraining factor in LIB advancement.

All-solid-state batteries (ASSBs) have emerged as a promising next-generation technology, expected to deliver higher energy and, in principle, power densities compared to conventional LIBs (Janek and Zeier, 2023; Lin et al., 2017; Schmuck et al., 2018). Unlike LIBs, ASSBs use solid electrolytes instead of organic liquid counterparts. This substitution can enhance long-term stability by preventing electrode cross-talk, an undesirable chemical interaction between dissolved active materials (Janek and Zeier, 2023). In addition, solid electrolytes can effectively reduce the risk of leakage, flammability and explosions, improving

overall thermal stability (Lin et al., 2017; Manthiram et al., 2017). The non-flammable nature or higher thermal thresholds of solid-state conductors prevents safety issues commonly associated with the high reactivity of liquid electrolytes (Lin et al., 2017). In this respect, the adoption of solid electrolytes enables the safe use of thin lithium (Li) metal anodes, which are otherwise limited by detrimental formation and growth of inhomogeneous deposits during Li plating/stripping reactions that often result in cell internal short-circuit with potentially disruptive consequences (e.g. thermal runaway, fire) in presence of organic liquid electrolytes. The use of thin Li metal anode is particularly attractive for next-generation battery designs, as Li offers much higher volumetric and gravimetric capacities than graphite, thus addressing the anode capacity limitations of traditional LIBs and further enhancing the ultimate cell output voltage (Boaretto et al., 2021; Janek and Zeier, 2023; Schmuck et al., 2018).

The all-solid-state design facilitates the integration of bipolar electrodes, allowing multiple battery cells to be stacked within a single package. This configuration enhances output voltage, reduces overall package volume, and consequently increases both energy density and storage efficiency (Hu, 2016). However, several challenges remain for the large-scale production of solid-state electrolytes. These include the need for inert processing environments for sulfides, high sintering temperatures for oxides, limited Li-ion conductivity at solid-state

\* Corresponding author.

E-mail addresses: [shan.zhang@chalmers.se](mailto:shan.zhang@chalmers.se), [zhangshan253@gmail.com](mailto:zhangshan253@gmail.com) (S. Zhang).

<https://doi.org/10.1016/j.jclepro.2025.146607>

Received 8 October 2024; Received in revised form 20 July 2025; Accepted 9 September 2025

Available online 13 September 2025

0959-6526/© 2025 The Authors. Published by Elsevier Ltd. This is an open access article under the CC BY license (<http://creativecommons.org/licenses/by/4.0/>).

| Abbreviations |  |        |   |
|---------------|--|--------|---|
| ASSB          | All-solid-state battery  | LIB    | Lithium-ion battery   |
| CCS           | Carbon Capture and Storage   | NCA    | Lithium Nickel Cobalt Aluminum Oxide<br>( $\text{LiNi}_{0.8}\text{Co}_{0.15}\text{Al}_{0.05}\text{O}_2$ ) |
| CMC           | Carboxymethyl cellulose  | NDCs   | Nationally determined contributions   |
| DMC           | Dimethyl carbonate   | NMC811 | Lithium Nickel Manganese Cobalt Oxide<br>( $\text{LiNi}_{0.8}\text{Mn}_{0.1}\text{Co}_{0.1}\text{O}_2$ )  |
| EC            | Ethylene carbonate   | pLCI   | Prospective life cycle inventory  |
| EVs           | Electric vehicles  | pLCA   | Prospective life cycle assessment   |
| ESW           | Electrochemical stability window   | PEO    | Polyethylene Oxide  |
| FU            | Functional unit  | PE     | polyethylene  |
| GHG           | Greenhouse gas   | PET    | Polyethylene terephthalate  |
| GWP           | Global warming potential   | PP     | Polypropylene   |
| IAM           | Integrated assessment model  | PVDF   | Polyvinylidene fluoride   |
| LCI           | Life cycle inventory   | SSB    | Solid-state battery   |
| LFP           | Lithium iron phosphate   | SSP2   | Shared Socioeconomic Pathway narrative 2  |
| LiTFSI        | lithium bis(trifluoromethanesulfonyl)imide/ $\text{LiN}(\text{SO}_2\text{CF}_3)_2$     | SBR    | Styrene-butadiene rubber  |
| LLZO          | Lithium Lanthanum Zirconium Oxide ( $\text{Li}_7\text{La}_3\text{Zr}_2\text{O}_{12}$ ) | TRL    | Technology readiness level  |

interfaces and the mechanically fragile nature of ceramic electrolytes, which are incompatible with established "roll-to-roll" manufacturing techniques (Cao et al., 2019; Frith et al., 2023; Xu et al., 2021). Despite these limitations, ongoing research continues to address these issues to improve the performance, scalability, and cost-effectiveness of ASSBs. Nonetheless, concerns remain regarding their long-term reliability, durability, and projected cost competitiveness.

Industry leaders such as Samsung, Solid Power, QuantumScape, and Toyota have made notable progress in advancing solid-state battery (SSB) technologies. Experimental data show that SSBs using NCA cathodes with Li metal anodes can achieve specific energies of up to 393 Wh/kg and volumetric energy densities of 1143 Wh/L, substantially higher than those of conventional LIBs (NCA vs. graphite), which typically reach 265 Wh/kg and 635 Wh/L, respectively (Janek and Zeier, 2023). Lithium-based SSBs are generally categorized into two types based on their electrolyte materials: ceramic and polymer. Ceramic electrolytes can be further divided into sulfide- and oxide-based systems. Both ceramic and polymer electrolytes exhibit different pros and cons. For example, ceramic garnet-type LLZO ( $\text{Li}_7\text{La}_3\text{Zr}_2\text{O}_{12}$ ) is favored for its high ionic conductivity, and compatibility with Li metal anodes due to its wide electrochemical stability window (ESW) and high shear modulus. The polymer electrolyte such as PEO (polyethylene oxide) with dissolved lithium bis(trifluoromethylsulfonyl)imide (LiTFSI) salt, is on the other hand preferred due to its ease of processing and capability to buffer electrode volume changes during battery operation (Tang et al., 2021; Zhao et al., 2020). Commercial demonstrations have shown promising performance at both cell and pack levels for SSBs featuring PEO-LiTFSI electrolytes with  $\text{LiFePO}_4$  cathodes (Wan et al., 2019).

Given their high raw material costs and complex processing requirements, ceramic-based ASSBs are expected to initially target premium market segments, such as high-end vehicles (Schmaltz et al., 2022), while polymer-based ASSBs are primarily intended for car-sharing services and buses (Song et al., 2023). Current research suggests that polymer-based SSBs are likely to reach commercialization first, followed by oxide- and sulfide-based SSBs (Schmaltz et al., 2022). Evaluating the potential environmental impacts of these emerging ASSBs is essential. Several life cycle assessment (LCA) studies have focused on ASSBs with sulfide-based electrolytes (Liu et al., 2024; Popien et al., 2023), oxide-based electrolytes (Lastoskie and Dai, 2015; Liu et al., 2024; Smith et al., 2021; Troy et al., 2016; Zhang et al., 2022), and polymer-based electrolyte (Vandepaer et al., 2017). Other studies have addressed solid electrolyte materials (Larrabide et al., 2022) and manufacturing technologies (Keshavarzmohammadian et al., 2018). However, due to limited data availability, most LCAs are conducted at the laboratory scale. Inventory data are often sources from different

references without consistent assumptions regarding battery size, geometry, and performance, leading to challenges in comparing different battery chemistries. In particular, inconsistencies in material composition and battery performance result in mismatches, as performance metrics are linked to the types and quantities of materials used.

Moreover, no research has investigated the future climate impacts of ASSBs. To address this gap, the present study performs a prospective life cycle assessment (pLCA) of two representative ASSB chemistries with polymer-based and ceramic-based electrolyte to explore their potential climate impact in 2025, 2030, 2040, and 2050. The study integrates battery-dimensioning inputs and corresponding gravimetric and volumetric energy densities from our own developed model. The findings aim to inform the sustainable development and deployment of future ASSB technologies.

## 2. Materials and method

This section outlines the methodology and workflow of the study, beginning with an explanation of the life cycle assessment (LCA) methodology (Section 2.1), followed by scenario development, and life cycle inventory (LCI) analysis.

### 2.1. Overall approach

A prospective life cycle assessment was conducted using an attributional cutoff method to evaluate the future climate impact of two all-solid-state batteries (ASSBs) and to compare their impacts with those of two conventional lithium-ion batteries (LIBs). The functional unit (FU) is defined as 1 kWh of battery capacity. This study focuses solely on the climate impact since the employed integrated assessment model (IAM) REMIND to explore future scenarios is centered on changes in greenhouse gas (GHG) emissions (Baumstark et al., 2021). Due to the early-stage development of ASSBs, high uncertainties exist in their use phase and end-of-life treatment. Consequently, this study focuses on the climate impact performance associated with battery production. The system boundaries include raw material extraction, transportation, precursor production, battery component production, and battery manufacturing processes. The climate impact per FU is quantified using the following equation:

$$\text{Climate impact per FU} = \frac{\sum f_i \times IS_i}{\text{specific energy}} \quad (1)$$

where  $f_i$  represents the mass requirement for each battery component (in kg) or the energy required for manufacturing 1 kg of battery (in kWh per

kg), and  $IS_i$  denotes the impact score (in kg CO<sub>2</sub>-eq per kg of material or per kWh of energy) for producing each unit of battery component and energy. The climate impact is calculated using the IPCC 2021 (100-year timeframe) GWP characterization factors. The battery production is assumed to take place in Europe. The LCA software Activity Browser was used for modeling (Steubing et al., 2020).

## 2.2. Battery technologies

Two representative ASSBs were evaluated: one with an NMC811 cathode and pure Li anode using LLZO as the electrolyte (technology readiness level, TRL = 5), and one with an LFP cathode and pure Li anode using a PEO-LiTFSI polymer electrolyte (TRL 8). For comparison, two LIBs using the same cathode materials were also assessed. In these LIBs, graphite was used as the anode and LiPF<sub>6</sub> salt in EC/DMC solvents as the electrolyte.

All studied batteries are modeled in a pouch cell configuration, which is the preferred configuration for SSBs. Unlike cylindrical cells, pouch cells lack standardization in terms of weight and dimensions. Significant variations in both weight and size are observed, even among products from the same manufacturer (Azhari et al., 2020). This study adopts battery cell dimensions sourced from Lee et al. (2020) for the four battery chemistries considered to ensure a fair comparison.

A pouch cell comprises multiple repeating units encased in a flexible, lightweight casing made from layers of polypropylene (PP), aluminum (Al), and polyethylene terephthalate (PET). Each unit is composed of multiple layers of battery components. For ASSBs, a bipolar internal design is applied, while a double-sided electrode coating design is additionally evaluated in the Supplementary Material (Section 1 and 2; Tables S3, S4, S14). The repeating unit consists of a solid-state electrolyte layer between two electrodes, with the solid electrolyte also functions as a separator. In this design, the Li anode also serves as a current collector, thus eliminating the need for a copper current collector. However, an aluminum current collector foil remains necessary on the cathode side. In LIBs, each unit includes a cathode and an anode layer separated by a porous polymer separator to prevent direct electrode contact. Cathode and anode materials are coated on both side of aluminum (cathode) and copper (anode) current collectors, respectively. The liquid electrolyte fills the pores of the separator and the electrodes, facilitating ion transport during cycling. The amount of component materials is calculated based on active material mass loading (g/cm<sup>2</sup>), layer thicknesses, porosity, and material densities. The cell capacity (mAh), specific energy (Wh/kg), and volumetric energy density (Wh/L) are calculated based on the cathode active material capacity (mAh/g), total cathode material, average voltage of the cell, and the

total weight and volume of the battery cell (Kevin W et al., 2022). Detailed battery dimensioning calculations are provided in the Supplementary Materials (Section 1).

Given the variability in ASSB design at this early stage of development, two scenarios were considered to capture a range of future potential configurations: a baseline and an optimal scenario. These scenarios were informed by expert inputs from battery developers and relevant literature (Supplementary Materials, Tables S1–2). The compositions and technical details of the studied battery cells are presented in Table 1, Table 2, and Fig. 1.

## 2.3. Life cycle inventory and future scenarios

Material requirements for battery components are derived from the battery dimensioning model introduced in Section 2.2. Energy requirements for battery manufacturing are sourced from Degen et al. (2023). Inventory data for material production and associated emissions are collected from prospective LCI (pLCI) databases, whenever possible. These pLCI databases are generated by integrating outputs from IAM with LCI database ecoinvent using the Premise Python package (Sacchi et al., 2022). This approach generates future-oriented LCI databases for the years 2025, 2030, 2040, and 2050, reflecting anticipated developments aligned with the Shared Socioeconomic Pathway narrative 2 (SSP2) and two climate targets: nationally determined contributions (NDCs) and the Paris Agreement's 1.5 °C goal (Pkbudg500). SSP2 represents a continuation of historical development trends across social, economic, and technological dimensions (Riahi et al., 2017). These scenarios predict global mean surface temperature increases limited to 2.5 °C (NDCs) and 1.5 °C (Pkbudg500) by year 2100. Specifically, the REMIND model is used to simulate potential transformations in various sectors and regions (Baumstark et al., 2021), such as future electricity sources, fuel production technologies, efficiency improvements in energy- and material-intensive processes, the implementation of Carbon Capture and Storage (CCS), and shifts in market shares of material and energy carriers. These transformations are then applied to modify corresponding unit processes in the ecoinvent 3.9 cut-off database (Wernet et al., 2016) via Premise, generating prospective ecoinvent databases in the year 2025, 2030, 2040, and 2050. For data unavailable in pLCI databases, they are collected from the latest literature. Specifically, the production of solid electrolytes LLZO and PEO-LiTFSI is modeled following the processes described by Liang et al. (2023) and Shao et al. (2018). Energy consumption is estimated using the method introduced in Geisler et al. (2004). The inventory for LiTFSI is from Deng et al. (2017). The life cycle inventory is provided in the Supplementary Material (Section 3; Table S12–S13).

**Table 1**

Composition (wt.%) of studied battery cells. Li refers to pure lithium foil. G refers to graphite. CMC refers to carboxymethyl cellulose. SBR refers to styrene butadiene rubber, Super C65 is a high performance electronically conductive carbon black powder. PEO-LiTFSI refers to polyethylene oxide embedding lithium bis(trifluoromethylsulfonyl)imide as electrolyte salt. LLZO refers to Li<sub>7</sub>La<sub>3</sub>Zr<sub>2</sub>O<sub>12</sub>.

|                   |                         | ASSB LFP(PEO-LiTFSI) |                     | ASSB NMC811(LLZO) |                 | LIB LFP                     |                             | LIB NMC811                  |                             |
|-------------------|-------------------------|----------------------|---------------------|-------------------|-----------------|-----------------------------|-----------------------------|-----------------------------|-----------------------------|
|                   |                         | baseline             | optimal             | Baseline          | Optimal         | Baseline                    | Optimal                     | Baseline                    | Optimal                     |
| Anode             | Anode active material   | 5.5 % (Li)           | 4.4 % (Li)          | 4.0 % (Li)        | 2.4 % (Li)      | 25.5 % (G)                  | 22.6 % (G)                  | 38.8 % (G)                  | 29.9 % (G)                  |
|                   | Super C65               | –                    | –                   | –                 | –               | 0.5 %                       | 0.5 %                       | 0.8 %                       | 0.6 %                       |
|                   | CMC-SBR                 | –                    | –                   | –                 | –               | 0.5 %                       | 0.5 %                       | 0.8 %                       | 0.6 %                       |
| Cathode           | Cathode active material | 32.5 % (LFP)         | 52.1 % (LFP)        | 35.7 % (NMC811)   | 50.3 % (NMC811) | 34.6 % (LFP)                | 45.0 % (LFP)                | 29.8 % (NMC811)             | 43.4 % (NMC811)             |
|                   | Super C65               | 0.7 %                | 1.0 %               | 0.7 %             | 1.0 %           | 0.7 %                       | 0.9 %                       | 0.6 %                       | 0.9 %                       |
|                   | PVDF                    | 0.7 %                | 1.0 %               | 0.7 %             | 1.0 %           | 0.7 %                       | 0.9 %                       | 0.6 %                       | 0.9 %                       |
| Current Collector | Al foil                 | 11.9 %               | 11.9 %              | 8.7 %             | 6.5 %           | 4.7 %                       | 3.0 %                       | 3.3 %                       | 2.4 %                       |
|                   | Cu foil                 | –                    | –                   | –                 | –               | 13.0 %                      | 8.0 %                       | 9.2 %                       | 6.3 %                       |
| Electrolyte       |                         | 43.9 % (PEO-LiTFSI)  | 26.4 % (PEO-LiTFSI) | 47.7 % (LLZO)     | 37.0 % (LLZO)   | 12.4 % (LiPF <sub>6</sub> ) | 13.0 % (LiPF <sub>6</sub> ) | 10.4 % (LiPF <sub>6</sub> ) | 10.7 % (LiPF <sub>6</sub> ) |
| Separator         | PE/PP                   | –                    | –                   | –                 | –               | 4.8 %                       | 3.7 %                       | 3.4 %                       | 2.9 %                       |
| Cell container    | PET/Al/PP               | 4.8 %                | 2.9 %               | 2.4 %             | 1.6 %           | 2.6 %                       | 1.8 %                       | 2.2 %                       | 1.5 %                       |
| Total weight      |                         | 150 g                | 168 g               | 300 g             | 305 g           | 275 g                       | 262 g                       | 327 g                       | 324 g                       |

**Table 2**

Technical details of the studied pouch cell batteries under baseline and optimal scenarios.

|  | ASSB LFP (PEO-LiTFSI) |         | ASSB NMC811 (LLZO) |         | LIB LFP  |         | LIB NMC811 |         |
|--|-----------------------|---------|--------------------|---------|----------|---------|------------|---------|
|  | Baseline              | Optimal | Baseline           | Optimal | Baseline | Optimal | Baseline   | Optimal |
| Anode thickness (single layer, $\mu\text{m}$ )   | 30                    | 20      | 30                 | 20      | 70       | 49      | 42.5       | 63.5    |
| Cathode mass loading ( $\text{mg}/\text{cm}^2$ ) | 10                    | 13.3    | 15                 | 23.4    | 13.4     | 22.6    | 16.3       | 27.9    |
| Electrolyte thickness ( $\mu\text{m}$ )          | 100                   | 50      | 35                 | 30      | –        | –       | –          | –       |
| Voltage (V)                                      | 3.5                   | 3.5     | 4.15               | 4.15    | 3.2      | 3.2     | 3.57       | 3.57    |
| Cell capacity (Wh)                               | 26                    | 46      | 95                 | 136     | 46       | 57      | 74         | 107     |
| Specific energy (Wh/kg)                          | 171                   | 274     | 316                | 446     | 166      | 216     | 227        | 331     |
| Volumetric energy density (Wh/L)                 | 248                   | 443     | 916                | 1314    | 442      | 551     | 723        | 1031    |

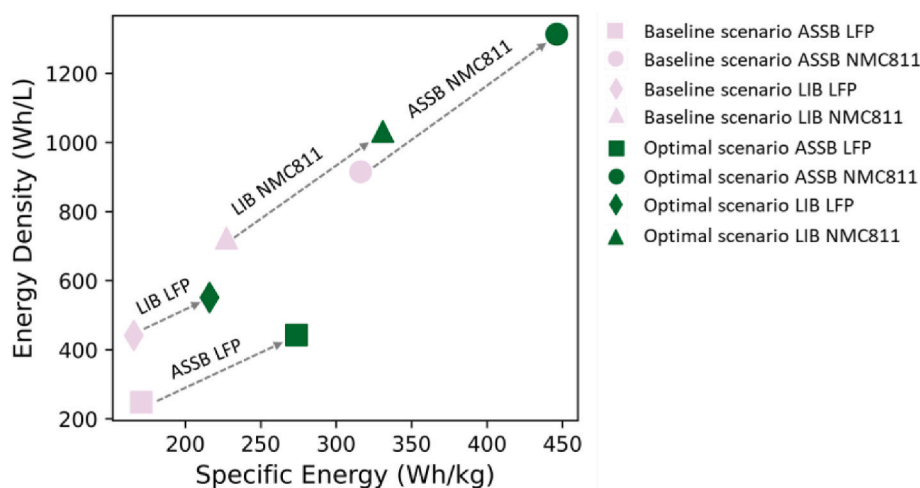


**Fig. 1.** Specific energy and volumetric energy density of the studied batteries. Light purple and green represent values produced from baseline and optimal battery design scenarios, respectively. Square, circle, diamond, and triangle markers refer to ASSB LFP (PEO-LiTFSI), ASSB NMC811 (LLZO), LIB LFP, and LIB NMC811, respectively. (For interpretation of the references to colour in this figure legend, the reader is referred to the Web version of this article.)

This study also considers the use of recycled battery materials by incorporating recycling content in the input materials. This consideration is in line with recent EU declaratives on the levels of recycled content for critical battery materials such as cobalt (Co), nickel (Ni), and lithium (REGULATION 2023/1542, 2023; Neef et al., 2021). Recycling content for aluminum (Al) (European Aluminium, 2022), copper (Cu) (Born and Giftci, 2024) and manganese (Mn) (Joint Research Centre, 2024) are also considered. These secondary materials are assumed to be sourced from recycled batteries and are utilized in the upstream processes of battery production, in forms of lithium carbonate, cobalt sulfate, nickel sulfate, manganese sulfate, Al (wrought alloy), as well as copper cathode (i.e., high-purity refined copper). Ultimately, they become part of the battery components such as cathode active material (NMC811 and LFP), Li foil anode, and electrolyte materials (PEO-LiTFSI, LLZO), as well as lithium hexafluorophosphate, aluminum and copper current collector foils, and aluminum pouch casings. Detailed assumptions on recycled contents and modified production processes are provided in the Supplementary Material (Section 2).

Combining two background scenarios (2.5 °C and 1.5 °C) with two battery design scenarios (baseline and optimal), four integrated scenarios are defined to explore the future climate impact of ASSBs, as shown in Table 3.

**Table 3**

Scenario combinations.

| Scenario names    | Background scenarios | Battery design scenarios |
|-------------------|----------------------|--------------------------|
| 2.5 °C - Baseline | SSP2-NDC             | Baseline design          |
| 1.5 °C - Baseline | SSP2-PkBudg500       | Baseline design          |
| 2.5 °C - Optimal  | SSP2-NDC             | Optimal design           |
| 1.5 °C - Optimal  | SSP2-PkBudg500       | Optimal design           |

### 3. Results and interpretation

This section is structured as follows: Section 3.1 uncovers the total climate impact of battery production across year 2025, 2030, 2040, and 2050, while Section 3.2 analyzes the relative contributions of battery materials and energy flows to the total climate impact of batteries.

#### 3.1. Climate impact

In 2025, ASSB NMC811 (LLZO) exhibits the highest climate impact among studied batteries, ranging from 42 to 71 kg CO<sub>2</sub>-eq/FU (Fig. 2). The climate impact of ASSB LFP (PEO-LiTFSI) ranges from 31 to 65 kg CO<sub>2</sub>-eq/FU, showing potential comparability with that of LIB NMC811 (29–41 kg CO<sub>2</sub>-eq/FU) and LIB LFP (27–42 kg CO<sub>2</sub>-eq/FU). These values are lower than those reported in previous LCA studies, primarily due to differences in battery design, battery specific energy, production region, use of secondary materials (such as Li, Co, Ni, Al, Cu, and Mn), and the inclusion of projected decarbonization strategies under the 1.5 °C and 2.5 °C scenarios modeled by REMIND. Among existing LCA studies on ASSBs, polymer-based ASSBs remain relatively unexplored. Only one study reported GHG emissions of 70–98 kg CO<sub>2</sub>-eq/kWh for an ASSB with LFP cathode and Li anode, although the polymer electrolyte was not specified (Vandepaer et al., 2017). For ASSBs with LLZO electrolytes, a pioneering study by Troy et al. (2016) reported GHG emissions of 1045 kg CO<sub>2</sub>-eq/kWh for an ASSB using LCO cathode and Li anode, which is up to 23 times higher than our results. The high value was mainly due to the non-optimized battery design, leading to high proportion of non-active materials and low specific energy (87 W h/kg). Liu et al. (2024) analyzed an ASSB cell (310 W h/kg) with an LFP cathode, Li anode and LLZO electrolyte, estimating a climate impact of approximately 133 kg CO<sub>2</sub>-eq/kWh.



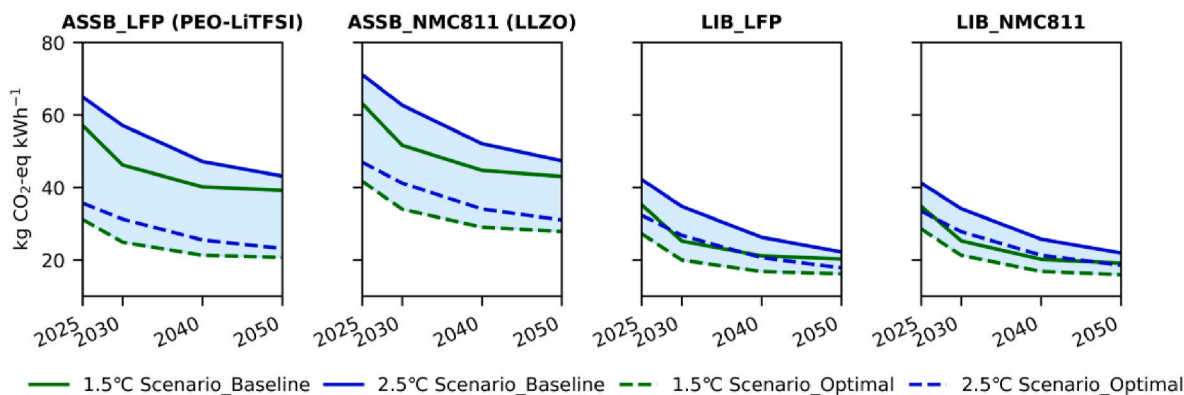


**Fig. 2.** Climate impact results per kWh of battery capacity for studied batteries at different years under four distinctive scenarios. The shaded blue area illustrates the disparity in climate impacts resulting from different scenarios. (For interpretation of the references to colour in this figure legend, the reader is referred to the Web version of this article.)

From 2025 onward, the climate impact is expected to decrease across all battery types due to increasing decarbonization under both 1.5 °C and 2.5 °C scenarios. By 2050, the projected reductions relative to 2025 are: 31–35 % for ASSB LFP (PEO-LiTFSI), 32–34 % for ASSB NMC811 (LLZO), 41–47 % for LIB LFP, and 44–47 % for LIB NMC811. Consequently, the projected 2050 climate impacts are 21–43 kg CO<sub>2</sub>-eq/FU (ASSB LFP), 28–47 kg CO<sub>2</sub>-eq/FU (ASSB NMC811), and 16–22 kg CO<sub>2</sub>-eq/FU for both LIB chemistries. These findings align with previous studies using prospective LCA methods (Xu et al., 2020; Zhang et al., 2024). These reductions are largely driven by decarbonization of the electricity sector. According to REMIND, the share of renewable energy in European electricity generation increases from 58 % to 96 % (2.5 °C scenario) and from 67 % to 97 % (1.5 °C scenario) between 2025 and 2050. As a result, the climate impact of medium-voltage electricity in Europe declines from 107 to 157 g CO<sub>2</sub>-eq/kWh in 2025 to 13.6–22 g CO<sub>2</sub>-eq/kWh in 2050. Additional reductions come from broader adoption of CCS in industrial power and heat generation, as well as the increased integration of recycled materials, particularly for high-emission metals.

Variation in the climate impact of ASSBs (represented by shaded ranges in Fig. 2) is primarily due to uncertainties in future battery design. Optimized designs reduce emissions by 45–47 % for ASSB LFP (PEO-LiTFSI), 34–35 % for ASSB NMC811 (LLZO), 20–23 % for LIB LFP, and 15–19 % for LIB NMC811, independent of year or scenario. Stronger climate targets (1.5 °C) and higher recycling rates can reduce emissions by 9–20 % for ASSB LFP (PEO-LiTFSI), 9–18 % for ASSB NMC811 (LLZO), 9–27 % for LIB LFP, and 13–26 % for LIB NMC811.

These findings suggest that for ASSBs, design optimization is a more effective strategy for climate impact reduction than stricter climate targets or mineral circularity at this early development stage. In contrast, this does not apply to LIBs, as their design is relatively mature and has almost approached its limits for further improvement. This highlights the critical importance of design innovation in the early stages of emerging battery technologies.

### 3.2. Contribution analysis of studied batteries

Fig. 3 illustrates the contribution analysis under the four scenarios. Total climate impact is divided into contributions from component production (including cathode active material, anode active material, current collectors for both electrodes, and electrolyte), battery manufacturing energy, and other components (e.g., binders, conductive additives, battery casing, etc.). Since battery design is assumed constant over time, design scenarios only affect the overall climate impact and the relative contributions of material and energy flows at a given year. The overtime changes in relative contributions arise solely from background scenarios (e.g. climate targets and recirculating minerals).

Solid electrolytes (PEO-LiTFSI and LLZO) are the main contributors to the climate impact of ASSBs, accounting for 28–55 % in ASSB LFP and 48–67 % in ASSB NMC811 across all years and scenarios. These environmental hotspots are consistent with earlier studies (Mandade et al., 2023). The high contribution arises from both their high production emissions (8–10 kg CO<sub>2</sub>-eq/kg for PEO-LiTFSI; 19–27 kg CO<sub>2</sub>-eq/kg for LLZO) and their substantial mass fractions (26–44 wt% in ASSB LFP and 37–48 wt% in ASSB NMC811), compared to only 10–13 wt% for liquid electrolytes in LIBs (Table 1).

Within PEO-LiTFSI, LiTFSI production contributes up to 84 % of total emissions, while methyl chloride accounts for up to 27 %. Although LiTFSI is the most widely used salt due to its solubility in PEO and good ionic conductivity, it is not indispensable. Alternative electrolyte salts could be explored to lower the climate impact. For instance, Wickerts et al. (2023) reported a 60 % climate impact reduction in lithium-sulfur batteries by replacing LiTFSI. For LLZO, lanthanum oxide production is the major contributor, accounting for up to 90 % of its emissions, with significant inputs from precursor materials such as citric acid, ammonium sulfate, and ammonium bicarbonate.

Cathode active materials also play a crucial role, contributing 13–26 % of the total impact for ASSB LFP (PEO-LiTFSI) and 19–36 % for ASSB NMC811 (LLZO). Their contribution is even more significant in LIBs, at 24–37 % for LIB LFP and 48–63 % for LIB NMC811. The impact of NMC811 is associated to the extraction of minerals and processing of materials like nickel sulfate, cobalt sulfate, and lithium hydroxide (Xu et al., 2022).

Li foil, used as the anode in ASSBs, contributes 14–27 % of the total emissions in ASSB LFP (PEO-LiTFSI) and 3–10 % in ASSB NMC811 (LLZO), despite comprising only 4.4–5.5 wt% and 2.4–4 wt% of these batteries. The future climate impact of Li production is 18–55 kg CO<sub>2</sub>-eq/kg, with up to 78 % of that attributed to lithium chloride (LiCl) production, and the remainder to electricity use in electrolysis. This high impact is due to the large amount of LiCl required for pure Li production, with 6.6 kg of LiCl needed to produce per kg of Li. Battery manufacturing energy use contributes 3–7 % of total ASSB emissions, varying by year and scenario, but plays a larger role in LIBs, particularly for LIB LFP, where it accounts for 14–27 % of the total emissions. The Al current collector contributes 9–12 % in ASSB LFP (PEO-LiTFSI) and 3–4 % in ASSB NMC811 (LLZO).

Battery design changes have significant effects on climate impact contributions. In ASSB LFP (PEO-LiTFSI), optimal design reduces electrolyte contribution from 41–55 % to 28–39 %, while increasing cathode impact from 13–14 % to 24–26 %. In ASSB NMC811(LLZO), optimal design reduces electrolyte contributions from 58–67 % to 48–57 %, while cathode contribution rises from 19–24 % to 29–36 %. This can mainly be attributed to the reduced electrolyte thickness. A similar finding was also indicated in Zhang et al. (2022). Between 2020 and

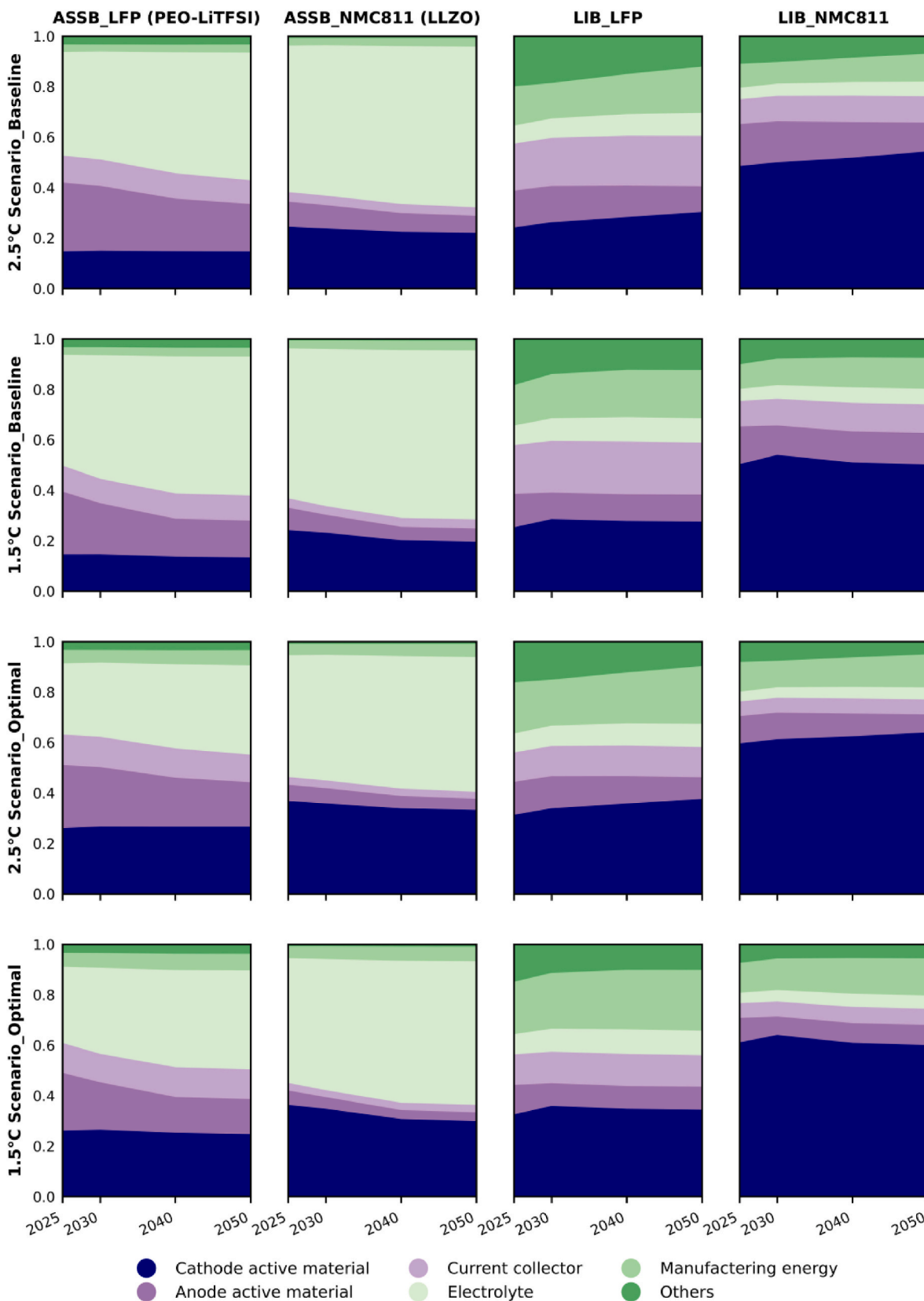


Fig. 3. Relative contributions of battery materials and energy use to the overall climate impact for four battery types under four scenarios. The scenarios consider changes in future battery design, energy-intensive production processes, and the use of secondary materials.

2050, electrolyte contributions increase slightly (e.g. 5–8 % in ASSB NMC811; 6–11 % in ASSB LFP), while anode and cathode active materials contributions decline (e.g., 7–10 % decrease in anode impact in ASSB LFP). These results illustrate how evolving battery designs, decarbonized supply chains, and recirculate materials dynamically reshape the environmental profile of next-generation batteries.

#### 4. Discussion

Previous studies have reported that the GHG emissions associated with ASSBs are generally higher than those of LIBs, largely due to the early development stage of ASSB technologies (Mandade et al., 2023). This study showed that even with future technology improvements and potential changes in the background production processes (for both ASSBs and LIBs), the climate impact of ASSBs with PEO-LiTFSI and LLZO electrolytes are likely to remain higher or at best comparable to that of LIBs.

Comparing the optimal battery design to the baseline, the specific energy increased by 60 % for ASSB LFP (PEO-LiTFSI) and by 47 % for ASSB NMC811 (LLZO). In the baseline design scenario, the ASSBs' specific energy fall below market expectations, while the optimal designs meet or exceed the projected expectations (Table 2). Previous studies have discussed that the market expects a minimum specific energy requirement of 350 W h/kg for the first generation of commercial ASSB (Frith et al., 2023; Schmaltz et al., 2022; Tian et al., 2021), with the potential for increasing this value in future designs (Randau et al., 2020). This suggests that the climate impact of ASSBs is more likely to fall into the lower range and has the potential to be reduced beyond the values reported in this study.

It is important to note that the parameters employed in the optimal design scenario represent potential achievable designs under current technological conditions rather than the performance limits of these battery technologies. By reducing the electrolyte layer thickness to reported minimal values (20  $\mu\text{m}$  for LLZO and 25  $\mu\text{m}$  for polymer-based electrolytes) (Kravchuk et al., 2021; Lennartz et al., 2023), while keeping other parameters constant, our model suggests that ASSBs could achieve climate impacts close to those of LIBs (see the shaded pink area in Fig. 4), although not necessarily lower.

The discussion above highlights the substantial climate benefits achievable through optimized battery design. Measures such as increasing cathode mass loading/areal capacity and reducing the thickness of non-active components including the electrolyte, anode, current collector, and cell casing, can significantly reduce both GHG emissions and material uses. These design modifications also increase energy density, further reducing climate impact per FU.

Optimized designs not only reduce environmental burden but may also offer economic advantages through lower material input amount.

Moreover, higher energy density aligns with market needs such as longer driving ranges. However, achieving such designs may require more advanced manufacturing infrastructure and greater capital investment, especially to handle the precision and stability required for thin-layer solid electrolytes and anode foil. Despite the potential trade-offs, these improvements could facilitate market entry, especially if cost parity with LIBs is achieved through economies of scale, which some forecasts suggest could occur as early as 2030 (Thomas et al., 2024).

This study has several limitations. First, the analysis focuses on battery cells and does not extend to the battery pack level. Solid-state electrolytes generally offer greater thermal stability compared to liquid electrolytes, reducing the need for active thermal management systems. This could result in higher specific energy at the pack-level and, consequently, lower climate impacts per FU. Furthermore, improved thermal stability can enhance performance under extreme operating conditions, including high temperatures, which can thereby aid fast charging. Second, this study does not account for the battery use phase. ASSBs are expected to follow different degradation mechanisms than LIBs and may offer longer cycle life due to the reduced degradation mechanisms such as electrolyte decomposition, electrode dissolution, and other side reactions. While some reports suggest that ASSBs can retain 90 % of their capacity after 5000 cycles (Crawford, 2022), expert opinion within the author team remains cautious due to concerns about energy efficiency, Coulombic efficiency, as well as the mechanical fragility of the solid electrolyte, under harsh operation conditions and especially vibrations. Further studies are needed to evaluate real-world durability.

To provide a more comprehensive view of the environmental performance of the ASSBs, we roughly estimated use-phase GHG emissions. It was assumed that ASSB NMC811 and LIB NMC811 are used in SUVs with 100 kWh battery packs, while ASSB LFP and LIB LFP are used in electric buses with 400 kWh battery packs. Using a FU of 1 kWh of stored energy over the battery's lifetime, results indicate that the use-phase emissions of ASSBs can be comparable to those of LIBs. When comparing use-phase and production-related emissions, ASSB NMC811 shows a use-phase impact equivalent to 0.5–0.9 times its production emissions, while for ASSB LFP the ratio ranges from 1.3 to 2.8 under the studied scenarios. Detailed assumptions and calculations are provided in Supplementary Material (Section 4).

While this study focuses on climate impact, it is also important to consider the potential impacts associated with the use of critical elements in ASSBs, such as pure lithium for anodes and rare earth elements in solid electrolytes. To address this, calculations were conducted on the raw materials required for producing ASSB-powered EVs between 2030 and 2035, based on EV sales projections under the IEA's Announced Pledges Scenario (IEA, 2024). It was assumed that 10 % of light-duty EVs would be powered by the ASSB NMC811 (LLZO), and 50 % of electric

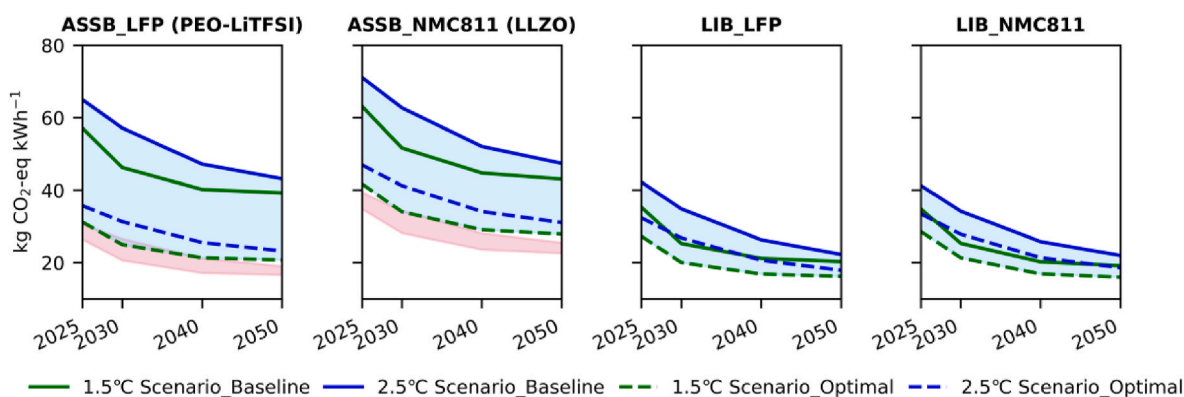


Fig. 4. Climate impact results per kWh of battery capacity for studied batteries at different years under four distinctive scenarios. The shaded pink area illustrates the climate impact of ASSBs using an extra thin electrolyte layer. (For interpretation of the references to colour in this figure legend, the reader is referred to the Web version of this article.)

buses sold would be powered by the ASSB LFP (PEO-LiTFSI) during this period (Detailed assumptions in Supplementary material, Section 4). The results suggest that light-duty EVs and electric buses powered by ASSBs demand more lithium, lanthanum, and zirconium, while requiring less Ni, Mn, and Co than LIBs would need to provide the same service (Table S19 in Supplementary Material). Compared to current global annual production levels, the additional demand for lithium, lanthanum, and zirconium corresponds to 3.3 times, 41.5 times, and 76 % of current global annual production, respectively. These findings thus highlight the need to critically assess whether the raw materials for these chemistries can be made available at scale, especially for lanthanum. To ensure long-term sustainability, it is essential to improve material efficiency in battery design, scale up mining and processing capacity for critical ASSB materials, and advance high-efficiency recycling technologies. From a technological standpoint, recycling methods for ASSBs are still in early stages of development and will require further research and industrial investment to scale. While some preliminary routes show promise, most existing recycling infrastructure is not currently equipped to efficiently handle ASSB-specific materials (Ahuis et al., 2024).

Although the EU has regulations for the mandatory recycling of critical minerals within batteries, these currently do not cover rare earth elements. With over 80 % of rare earth elements being mined and processed in China, and considering the projected demand for these materials in all-solid-state batteries (ASSBs), it is crucial to include them in regulatory frameworks to ensure a resilient supply chain. Advancing specialized recycling technologies and establishing regulatory mechanisms tailored to solid-state chemistries will therefore be essential to enable circularity in the ASSB value chain.

Driven by market demand and investment, particularly in regions such as North America where high-range EVs are preferred, the development of solid-state batteries has become an inevitable aspect of technological progress (IEA, 2024). To reduce their overall climate impact and support responsible growth, the following strategies should be prioritized.

Therefore, continuous efforts to refine the material production processes and enhance the material efficiency of solid-state batteries are needed to reduce their overall climate impact. Based on our analysis, feasible strategies for achieving sustainable development in ASSBs are:

1. Improving battery design by reducing the thickness of non-cathode layers and increasing cathode areal capacity.
2. Decarbonizing production processes, especially for solid electrolyte materials, by developing cleaner methods, exploring alternative materials, and integrating CCS technologies.
3. Increasing the recycling systems, especially for rare earth elements. Enhancing recycling within the EU can strengthen the supply chain, reduce dependency on primary extraction and climate impact.

Policy and regulatory support can play a key role in this transition. Existing frameworks may need to be extended or updated to address rare earth elements used in ASSBs. Additionally, policies that incentivize the use of renewable energy and impose stricter standards on emissions can drive the industry towards more sustainable practices.

The scope of this study focuses on climate impacts associated with battery production in Europe. Caution is needed when generalizing these results to other regions. The climate impact of ASSBs can vary significantly depending on the electricity mix used in battery manufacturing and the pace of regional decarbonization. For example, under the 2.5 °C scenario in 2025, approximately 33 % of the U.S. electricity mix is sourced from gas, 43 % of China's electricity comes from coal, and only 21 % of electricity in Europe is generated from fossil fuels (including gas, coal, and oil).

## 5. Conclusions

Based on the functional unit of 1 kWh of battery capacity, ASSB

NMC811 (LLZO) presents a higher climate impact than lithium-ion batteries (LIBs), while ASSB LFP (PEO-LiTFSI) shows the potential for a comparable climate impact to LIBs. Optimizing battery design can significantly reduce the climate impact of ASSBs. The solid-state electrolyte and cathode active materials are main contributors to the climate impact of both ASSBs, with the anode and current collector being particularly significant in polymer-based ASSBs. From 2025 to 2050, the climate impact of all studied batteries is expected to decrease due to decarbonization efforts and the increased use of secondary materials. Key strategies for reducing the climate impact of ASSBs include optimizing battery design such as minimizing the weight of non-cathode layers, replacing high impacts materials, and developing cleaner production processes. The results also indicate that for studied ASSBs, battery design improvements may have a more significant influence on reducing the climate impact than enhancements in upstream production processes (such as decarbonization of energy intensive processes and use of secondary materials). The large-scale development of ASSBs also requires careful assessment of their material demand.

## CRedit authorship contribution statement

**Shan Zhang:** Writing – review & editing, Writing – original draft, Visualization, Software, Methodology, Investigation, Formal analysis, Conceptualization. **Daniel Brandell:** Writing – review & editing, Investigation. **Mario Valvo:** Writing – review & editing, Investigation. **Bernhard Steubing:** Writing – review & editing. **Åke Nordberg:** Writing – review & editing, Supervision.

## Declaration of competing interest

The authors declare that they have no known competing financial interests or personal relationships that could have appeared to influence the work reported in this paper.

## Acknowledgements

This work was supported by STandUp for Energy program, and the Department of Energy and Technology, Swedish University of Agricultural Sciences.

## Appendix A. Supplementary data

Supplementary data to this article can be found online at <https://doi.org/10.1016/j.jclepro.2025.146607>.

## Data availability

Data will be made available on request.

## References

- Ahuis, M., Doose, S., Vogt, D., Michalowski, P., Zellmer, S., Kwade, A., 2024. Recycling of solid-state batteries. *Nat. Energy* 9 (4), 373–385. <https://doi.org/10.1038/s41560-024-01463-4>.
- Azhari, L., Bong, S., Ma, X., Wang, Y., 2020. Recycling for all solid-state lithium-ion batteries. *Matter* 3 (6), 1845–1861.
- Baumstark, L., Bauer, N., Benke, F., Bertram, C., Bi, S., Gong, C.C., Dietrich, J.P., Dirmaichner, A., Giannousakis, A., Hilaire, J., Klein, D., Koch, J., Leimbach, M., Levesque, A., Madeddu, S., Malik, A., Merfort, A., Merfort, L., Odenweller, A., Luderer, G., 2021. REMIND2.1: transformation and innovation dynamics of the energy-economic system within climate and sustainability limits. *Geosci. Model Dev. (GMD)* 14 (10), 6571–6603. <https://doi.org/10.5194/gmd-14-6571-2021>.
- Boaretto, N., Garbayo, I., Valiyaveetil-SobhanRaj, S., Quintela, A., Li, C.M., Casas-Cabanas, M., Aguesse, F., 2021. Lithium solid-state batteries: state-of-the-art and challenges for materials, interfaces and processing. *J. Power Sources* 502. <https://doi.org/10.1016/j.jpowsour.2021.229919>.
- Born, K., Ciftci, M.M., 2024. The limitations of end-of-life copper recycling and its implications for the circular economy of metals. *Resour. Conserv. Recycl.* 200, 107318.



- Cao, Y.L., Li, M., Lu, J., Liu, J., Amine, K., 2019. Bridging the academic and industrial metrics for next-generation practical batteries. *Nat. Nanotechnol.* 14 (3), 200–207. <https://doi.org/10.1038/s41565-019-0371-8>.
- Crawford, M., 2022. Solid-state batteries drive the future of the EV market. <https://www.asme.org/topics-resources/content/solid-state-batteries-drive-the-future-of-the-ev-market>.
- Degen, F., Winter, M., Bendig, D., Tübke, J., 2023. Energy consumption of current and future production of lithium-ion and post lithium-ion battery cells. *Nat. Energy* 1–12.
- Deng, Y.L., Li, J.Y., Li, T.H., Gao, X.F., Yuan, C., 2017. Life cycle assessment of Lithium sulfur battery for electric vehicles. *J. Power Sources* 343, 284–295. <https://doi.org/10.1016/j.jpowsour.2017.01.036>.
- European Aluminium, 2022. EUROPEAN aluminium VISION 2050: a vision for strategic, low carbon and competitive aluminium. [https://european-aluminium.eu/wp-content/uploads/2022/10/sample\\_vision-2050-low-carbon-strategy\\_20190401.pdf](https://european-aluminium.eu/wp-content/uploads/2022/10/sample_vision-2050-low-carbon-strategy_20190401.pdf).
- Frith, J.T., Lacey, M.J., Ulissi, U., 2023. A non-academic perspective on the future of lithium-based batteries. *Nat. Commun.* 14 (1), 420.
- Geisler, G., Hofstetter, T.B., Hungerbühler, K., 2004. Production of fine and speciality chemicals: procedure for the estimation of LCIs. *Int. J. Life Cycle Assess.* 9 (2), 101–113. <https://doi.org/10.1007/Bf02978569>.
- Hu, Y.-S., 2016. Batteries: getting solid. *Nat. Energy* 1 (4), 1–2.
- IEA, 2024. Global EV outlook 2024. <https://iea.blob.core.windows.net/assets/a9c3544b-0b12-4e15-b407-65f5c8ce1b5f/GlobalEVOutlook2024.pdf>.
- Janek, J., Zeier, W.G., 2023. Challenges in speeding up solid-state battery development. *Nat. Energy* 8 (3), 230–240. <https://doi.org/10.1038/s41560-023-01208-9>.
- Joint Research Centre, 2024. Lithium-based batteries supply chain challenges. <https://rmis.jrc.ec.europa.eu/analysis-of-supply-chain-challenges-49b749>.
- Keshavarzomohammadian, A., Cook, S.M., Milford, J.B., 2018. Cradle-to-gate environmental impacts of sulfur-based solid-state lithium batteries for electric vehicle applications. *J. Clean. Prod.* 202, 770–778. <https://doi.org/10.1016/j.jclepro.2018.08.168>.
- Kevin, W.K., Joseph, J.K., Paul, A. N., Shabbir, A., 2022. Battery Performance and Cost Modeling for Electric-Drive Vehicles.
- Kravchik, K.V., Okur, F., Kovalenko, M.V., 2021. Break-even analysis of all-solid-state batteries with Li-Garnet solid electrolytes. *ACS Energy Lett.* 6 (6), 2202–2207. <https://doi.org/10.1021/acsenenergylett.1c00672>.
- Larrabide, A., Rey, I., Lizundia, E., 2022. Environmental impact assessment of solid polymer electrolytes for solid-state lithium batteries. *Adv. Energy Sustain. Res.* 3 (10). <https://doi.org/10.1002/aesr.202200079>.
- Lastoskie, C.M., Dai, Q., 2015. Comparative life cycle assessment of laminated and vacuum vapor-deposited thin film solid-state batteries. *J. Clean. Prod.* 91, 158–169. <https://doi.org/10.1016/j.jclepro.2014.12.003>.
- Lee, Y.G., Fujiki, S., Jung, C.H., Suzuki, N., Yashiro, N., Omoda, R., Ko, D.S., Shiratsuchi, T., Sugimoto, T., Ryu, S., Ku, J.H., Watanabe, T., Park, Y., Aihara, Y., Im, D., Han, I.T., 2020. High-energy long-cycling all-solid-state lithium metal batteries enabled by silver-carbon composite anodes (vol 171, pg 568, 2020). *Nat. Energy* 5 (4), 348. <https://doi.org/10.1038/s41560-020-0604-y>, 348.
- Lennartz, P., Paren, B.A., Herzog-Arbeitman, A., Chen, X.C., Johnson, J.A., Winter, M., Shao-Horn, Y., Brunklaus, G., 2023. Practical considerations for enabling Li|polymer electrolyte batteries. *Joule* 7 (7), 1471–1495. <https://doi.org/10.1016/j.joule.2023.06.006>.
- Liang, Q., Chen, L., Tang, J., Liu, X., Liu, J., Tang, M., Wang, Z., 2023. Large-scale preparation of ultrathin composite polymer electrolytes with excellent mechanical properties and high thermal stability for solid-state lithium-metal batteries. *Energy Storage Mater.* 55, 847–856.
- Lin, D.C., Liu, Y.Y., Cui, Y., 2017. Reviving the lithium metal anode for high-energy batteries. *Nat. Nanotechnol.* 12 (3), 194–206. <https://doi.org/10.1038/Nnano.2017.16>.
- Liu, Z.Y., Li, X., Zhang, H.L., Huang, K., Yu, Y.J., 2024. Are solid-state batteries absolutely more environmentally friendly compared to traditional batteries-analyzing from the footprint family viewpoint. *J. Clean. Prod.* 447. <https://doi.org/10.1016/j.jclepro.2024.141452>.
- Mandate, P., Weil, M., Baumann, M., Wei, Z.X., 2023. Environmental life cycle assessment of emerging solid-state batteries: a review. *Chem. Eng. J. Adv.* 13. <https://doi.org/10.1016/j.cej.2022.100439>.
- Manthiram, A., Yu, X.W., Wang, S.F., 2017. Lithium battery chemistries enabled by solid-state electrolytes. *Nat. Rev. Mater.* 2 (4). <https://doi.org/10.1038/natrevmats.2016.103>.
- Neef, C., Schmalz, T., Thielmann, A., 2021. Recycling of Lithium-ion batteries: opportunities and challenges for mechanical and plant engineering. [https://www.isi.fraunhofer.de/content/dam/isi/dokumente/cct/2021/VDMA\\_Kurzstudie\\_Batterier recycling.pdf](https://www.isi.fraunhofer.de/content/dam/isi/dokumente/cct/2021/VDMA_Kurzstudie_Batterier recycling.pdf).
- Popien, J.L., Thies, C., Barke, A., Spengler, T.S., 2023. Comparative sustainability assessment of lithium-ion, lithium-sulfur, and all-solid-state traction batteries. *Int. J. Life Cycle Assess.* <https://doi.org/10.1007/s11367-023-02134-4>.
- Randau, S., Weber, D.A., Kotz, O., Koerver, R., Braun, P., Weber, A., Ivers-Tiffée, E., Adermann, T., Kulisch, J., Zeier, W.G., Richter, F.H., Janek, J., 2020. Benchmarking the performance of all-solid-state lithium batteries. *Nat. Energy* 5 (3), 259–270. <https://doi.org/10.1038/s41560-020-0565-1>.
- REGULATION (EU) 2023/1542, 2023. OF THE EUROPEAN Parliament and of the council. <https://eur-lex.europa.eu/legal-content/EN/TXT/HTML/?uri=CELEX%3A32023R1542>.
- Riahi, K., van Vuuren, D.P., Kriegler, E., Edmonds, J., O'Neill, B.C., Fujimori, S., Bauer, N., Calvin, K., Dellink, R., Fricko, O., Lutz, W., Popp, A., Cuaresma, J.C., Samir, K.C., Leimbach, M., Jiang, L.W., Kram, T., Rao, S., Emmerling, J., Tavoni, M., 2017. The shared socioeconomic pathways and their energy, land use, and greenhouse gas emissions implications: an overview. *Glob. Environ. Change-Hum. Pol. Dimens.* 42, 153–168. <https://doi.org/10.1016/j.gloenvcha.2016.05.009>.
- Sacchi, R., Terlouw, T., Siala, K., Dirmaichner, A., Bauer, C., Cox, B., Mutel, C., Daiglou, V., Luderer, G., 2022. PROspective EnvironMental impact asSEment (premise): a streamlined approach to producing databases for prospective life cycle assessment using integrated assessment models. *Renew. Sustain. Energy Rev.* 160. <https://doi.org/10.1016/j.rser.2022.112311>.
- Schmalz, T., Wicke, T., Weymann, L., Voß, P., Neef, C., Thielmann, A., 2022. Solid-State Battery Roadmap 2035+.
- Schmich, R., Wagner, R., Horpel, G., Placke, T., Winter, M., 2018. Performance and cost of materials for lithium-based rechargeable automotive batteries. *Nat. Energy* 3 (4), 267–278. <https://doi.org/10.1038/s41560-018-0107-2>.
- Shao, C., Ge, K., Wang, L., 2018. A kind of garnet of cubic phase containing aluminium Li7La3Zr2O12Preparation method. CN Patent No. CN109319837A). <https://patents.google.com/patent/CN109319837A/en>.
- Smith, L., Ibn-Mohammed, T., Astudillo, D., Brown, S., Reaney, I.M., Koh, S.C.L., 2021. The role of cycle life on the environmental impact of Li6.4La3Zr1.4Ta0.6O12 based solid-state batteries. *Adv. Sustain. Sys.* 5 (2). <https://doi.org/10.1002/adus.202000241>.
- Song, Z.Y., Chen, F.F., Martínez-Ibañez, M., Feng, W.F., Forsyth, M., Zhou, Z.B., Armand, M., Zhang, H., 2023. A reflection on polymer electrolytes for solid-state lithium metal batteries. *Nat. Commun.* 14 (1). <https://doi.org/10.1038/s41467-023-40609-y>.
- Steubing, B., de Koning, D., Haas, A., Mutel, C.L., 2020. The activity browser - an open source LCA software building on top of the brightway framework. *Softw. Impact.* 3. <https://doi.org/10.1016/j.simpa.2019.100012>.
- Tang, S., Guo, W., Fu, Y.Z., 2021. Advances in composite polymer electrolytes for lithium batteries and beyond. *Adv. Energy Mater.* 11 (2). <https://doi.org/10.1002/aenm.202000802>.
- Thomas, F., Mahdi, L., Lemaire, J., Santos, D.M.F., 2024. Technological advances and market developments of solid-state batteries: a review. *Materials* 17 (1). <https://doi.org/10.3390/ma17010239>.
- Tian, Y.S., Zeng, G.B., Rutt, A., Shi, T., Kim, H., Wang, J.Y., Koettgen, J., Sun, Y.Z., Ouyang, B., Chen, T.N., Lun, Z.Y., Rong, Z.Q., Persson, K., Ceder, G., 2021. Promises and challenges of next-generation "Beyond Li-ion" batteries for electric vehicles and grid decarbonization. *Chem. Rev.* 121 (3), 1623–1669. <https://doi.org/10.1021/acs.chemrev.0c00767>.
- Troy, S., Schreiber, A., Reppert, T., Gehrke, H.G., Finsterbusch, M., Uhlenbruck, S., Stenzel, P., 2016. Life cycle assessment and resource analysis of all-solid-state batteries. *Appl. Energy* 169, 757–767. <https://doi.org/10.1016/j.apenergy.2016.02.064>.
- Vandepaer, L., Cloutier, J., Amor, B., 2017. Environmental impacts of Lithium metal polymer and Lithium-ion stationary batteries. *Renew. Sustain. Energy Rev.* 78, 46–60. <https://doi.org/10.1016/j.rser.2017.04.057>.
- Wan, J.Y., Xie, J., Kong, X., Liu, Z., Liu, K., Shi, F.F., Pei, A., Chen, H., Chen, W., Chen, J., Zhang, X.K., Zong, L.Q., Wang, J.Y., Chen, L.Q., Qin, J., Cui, Y., 2019. Ultrathin, flexible, solid polymer composite electrolyte enabled with aligned nanoporous host for lithium batteries. *Nat. Nanotechnol.* 14 (7), 705. <https://doi.org/10.1038/s41565-019-0465-3>.
- Wernet, G., Bauer, C., Steubing, B., Reinhard, J., Moreno-Ruiz, E., Weidema, B., 2016. The ecoinvent database version 3 (part I): overview and methodology. *Int. J. Life Cycle Assess.* 21, 1218–1230.
- Wickerts, S., Arvidsson, R., Nordlöf, A., Svanström, M., Johansson, P., 2023. Prospective life cycle assessment of lithium-sulfur batteries for stationary energy storage. *ACS Sustain. Chem. Eng.* 11 (26), 9553–9563. <https://doi.org/10.1021/acscuschemeng.3c00141>.
- Xu, C., Dai, Q., Gaines, L., Hu, M., Tukker, A., Steubing, B., 2020. Future material demand for automotive lithium-based batteries. *Commun. Mater.* 1 (1), 1–10.
- Xu, L., Lu, Y., Zhao, C.Z., Yuan, H., Zhu, G.L., Hou, L.P., Zhang, Q., Huang, J.Q., 2021. Toward the Scale-Up of solid-state lithium metal batteries: the gaps between lab-level cells and practical large-format batteries. *Adv. Energy Mater.* 11 (4). <https://doi.org/10.1002/aenm.202002360>.
- Xu, C., Steubing, B., Hu, M., Harpprecht, C., van der Meide, M., Tukker, A., 2022. Future greenhouse gas emissions of automotive lithium-ion battery cell production. *Resour. Conserv. Recycl.* 187, 106606.
- Zhang, J.Y., Ke, X.Y., Gu, Y., Wang, F.N., Zheng, D.Y., Shen, K., Yuan, C., 2022. Cradle-to-gate life cycle assessment of all-solid-state lithium-ion batteries for sustainable design and manufacturing. *Int. J. Life Cycle Assess.* 27 (2), 227–237. <https://doi.org/10.1007/s11367-022-02023-2>.
- Zhang, S., Steubing, B., Potter, H.K., Hansson, P.A., Nordberg, A., 2024. Future climate impacts of sodium-ion batteries. *Resour. Conserv. Recycl.* 202. <https://doi.org/10.1016/j.resconrec.2023.107362>.
- Zhao, Q., Stalin, S., Zhao, C.Z., Archer, L.A., 2020. Designing solid-state electrolytes for safe, energy-dense batteries. *Nat. Rev. Mater.* 5 (3), 229–252. <https://doi.org/10.1038/s41578-019-0165-5>.